



Synthesis, Characterization and Photocatalytic Applications of Nanocomposites with Nickel Nitrate Doped Zinc Oxide Nanoparticles

ANTONY LAWRENCE ANDREWS^{1,✉}, M. PACKIYA RAJ^{2,✉}, ANAND GASPAR^{3,✉},
R. GOVINDARASU^{4,✉}, M. SATHISH^{5,*✉}, G. RAMALINGAM^{6,✉} and S. THIYAGARAJ^{7,✉}

¹Department of Physics, School of Natural and Physical Sciences, The University of Papua New Guinea, P. O. Box 320, Waigani Campus, Port Moresby, National Capital District 134, Papua New Guinea

²PG & Research Department of Physics, Loyola College, Chennai-600034, India

³PG & Research Department of Chemistry, St. Joseph's College of Arts and Science (Autonomous), Cuddalore-607001, India

⁴Department of Chemical Engineering, Sri Venkateswara College of Engineering, Sriperumbudur, Chennai-602117, India

⁵PG & Research Department of Physics, St. Joseph's College of Arts and Science (Autonomous), Cuddalore-607001, India

⁶Department of Nanoscience and Technology, Alagappa University, Karaikudi-630003, India

⁷Department of Physics & Electronics, School of Sciences, Jain University, Bangalore-560069, India

*Corresponding author: E-mail: sathishmary2013@gmail.com

Received: 2 March 2025;

Accepted: 17 April 2025;

Published online: 27 May 2025;

AJC-21999

In this work, the co-precipitation method was used to synthesize nickel nitrate-doped zinc oxide (Ni:ZnO) nanoparticles. Zinc oxide (ZnO) is widely known for its optical, electrical and catalytic properties, making it a versatile material in various applications, including sensors, catalysis and optoelectronic devices. The incorporation of nickel nitrate into the ZnO matrix aims to enhance its structural and functional properties by altering the defect states, band gap and surface morphology. In this study, Ni-doped ZnO nanoparticles were prepared using zinc nitrate as precursor for ZnO and nickel nitrate as the dopant. The doping concentration of nickel nitrate was varied to investigate its impact on the structural, optical and magnetic properties of the synthesized material. The co-precipitation method was employed, followed by calcination to achieve crystallization. The synthesized nanoparticles were characterized using X-ray diffraction (XRD), Fourier transform infrared (FTIR) spectroscopy, scanning electron microscopy (SEM) and UV-Vis spectroscopy. The results revealed that nickel doping significantly affected the crystallite size, bandgap energy and optical absorption properties of ZnO, making Ni:ZnO a promising candidate for potential applications in photocatalysis, cyclic voltammetry provides insights into its electrochemical properties and optoelectronics.

Keywords: Nickel doped ZnO, Co-precipitation, Optoelectronics, Photocatalytic applications, Cyclic voltammetry.

INTRODUCTION

Ni-ZnO is a potential composite material incorporating the advantages of nickel doping with the properties ZnO imparts such as a wide band gap, high exciton binding energy and excellent chemical stability. The presence of nickel ions in the ZnO lattice alters its electrical, optical and magnetic characteristics, thus increasing it for modern-day applications. Accordingly, the doping induced localized states and lowered the band gap for better absorption in the visible range which is of great necessity in photocatalytic and optoelectronic applications [1-5]. Materials like Ni-ZnO obtain a new life owing to their enhanced

electrical conductivity, vacancy engineering and possible room temperature ferromagnetic activity for applications in spintronic devices. The multifunctional characteristics render Ni-ZnO attractive to energy storage, gas sensing, photocatalysis and nonlinear optics applications, thus offering an efficient and green solution to future technological problems [6,7].

Nickel nitrate assumes prominence in catalyst preparation, ceramics and production of doped materials because of its uniform incorporation of nickel in host matrices. In addition, with its perennial properties, corrosion resistance and electroplating, nickel nitrate is a serious compounds for industrial applications [8,9]. NiO alone may promote advances in science and technol-

ogy aplenty be it with sensing, electronic devices to energy storage. On the contrary, ZnO being a versatile semiconductor possesses a band gap of nearly 3.37 eV. It has got vast optical, sensing and storage properties [10-13]. The wurtzite crystal structure and inherent defect chemistry of Zn give it high tunability for specific applications. The excellent optical application and piezoelectric properties of ZnO make the material vital for photocatalytic mechanism. Besides that, due to its biocompatibility and antimicrobial properties, it also finds applications in biomedical engineering. Moreover, the abundance, low cost and friendliness of ZnO make it even a more important sustainable material for new technology generations.

Nanocomposites are the materials formed with a matrix embedded with nanoscale fillers, providing special mechanical, chemical and physical specifications to the composites. Owing to their increased basal area, the fine characters and quantum regulations of such materials have yielded additional mechanical magnitude and durability in thermal treatment, electric conductance improvement and optimizing of optical features [14-16]. They are visible in diverse areas including energy storage, environmental cleanup, health, electronics and aerospace. These cone-style materials have steadily been contributing to modern material sciences in providing hallmark solutions to complex technical problems by combining and polishing the most important properties of multiple components at nano fascia. With these advantages in support of nanocomposites, nickel and zinc oxide was used in this study, which presents with the introduction of doped nickel nitrate in increasing its attributes [17-20]. The co-precipitation method was chosen for the synthesis of this nanocomposite. The synthesized nanocomposite structure, functional groups, optical property and the nature of the material were studied by the XRD, FT-IR and UV-Vis studies. Nickel nitrate-doped zinc oxide (Ni:ZnO) is a nanocomposite material that incorporates nickel ions into the crystal lattices of ZnO [21-23]. This modification has a profound effect on the material's physical and chemical properties and hence, increases its performance in various applications. Summarized, nickel nitrate-doped zinc oxide enchants a compatible conjoined effect of nickel with ZnO, enabling its better use to electronics, catalysis and sensing applications [24]. The electrochemical properties of Ni-doped ZnO, such as its charge storage and redox behaviour, are studied using cyclic voltammetry (CV). This work analyzes the provided CV plot and correlates it with the synthesis and characterization data.

EXPERIMENTAL

Nickel nitrate hexahydrate ($\text{Zn}(\text{NO}_3)_2 \cdot 6\text{H}_2\text{O}$); zinc nitrate hexahydrate ($\text{Zn}(\text{NO}_3)_2 \cdot 6\text{H}_2\text{O}$); ammonium hydroxide (NH_4OH) and sodium hydroxide (NaOH) were procured from Sigma-Aldrich, USA.

Preparation of stock solutions: To prepare stock solutions, dissolved 14.54 g of $\text{Ni}(\text{NO}_3)_2 \cdot 6\text{H}_2\text{O}$ into 100 mL of distilled water to obtain a 0.5 M solution. Dissolved 14.87 g of $\text{Zn}(\text{NO}_3)_2 \cdot 6\text{H}_2\text{O}$ in 100 mL of distilled water to obtain a 0.5 M solution. Prepared the mixtures of three molar ratios as follows: Pure ZnO, used 100 mL of zinc nitrate solution (no nickel nitrate). For Ni:Zn = 0.2:1, mixed 20 mL of nickel nitrate

solution with 80 mL of zinc nitrate. For Ni:Zn = 0.4:1, mixed 40 mL of nickel nitrate solution with 60 mL of zinc nitrate.

Procedure: For each solution mixture, added 0.5 M NH_4OH or NaOH dropwise with constant stirring using magnetic stirrer for 30 min by maintaining the pH of solution at 9-10. A pale-greenish precipitate was formed and at room temperature, the precipitate was allowed to settle undisturbed for 1 to 2 h. Then the precipitate was filtered and washed the precipitate several times until the filtrate is free of nitrates. The precipitate was dried in an oven at 100-120 °C for 12 h. In next step, the samples were calcined between 450-600 °C for 24 h. After calcination, the samples were grinded to fine powder using agate mortar and pestle.

RESULTS AND DISCUSSION

X-ray diffraction studies: The X-ray diffraction analysis showed significant insight into the crystalline structure as well as nickel-doping on the $\text{Zn}_{1-x}\text{Ni}_x\text{O}$ nanostructures. The diffraction patterns revealed the distinct peaks at 2θ values of 31.260°, 31.705°, 32.128°, 36.162°, 36.610°, 56.246° and 56.694°. These data clearly depict the hexagonal wurtzite ZnO crystal structure's distinctive planes in accordance with JCPDS card No. 36-1451 (Fig. 1). The observed peaks of high specificity confirm the high crystallinity of the synthesized samples. Small shifts of the peaks like shifts in (100), (101) and (110) planes are suggestive that substitution of Zn^{2+} ions (ionic radius 0.74 Å) by Ni^{2+} ions (ionic radius 0.69 Å) causes lattice strain and distortion. This substitution causes a slight reduction of the lattice parameters which one can observe in the systematic variation of the diffraction peaks. The peak 32.128° accounts for the (100) plane, while that of 36.162° and 36.610° can be attributed to the (101) plane, while the peaks 56.246° and 56.694° correspond

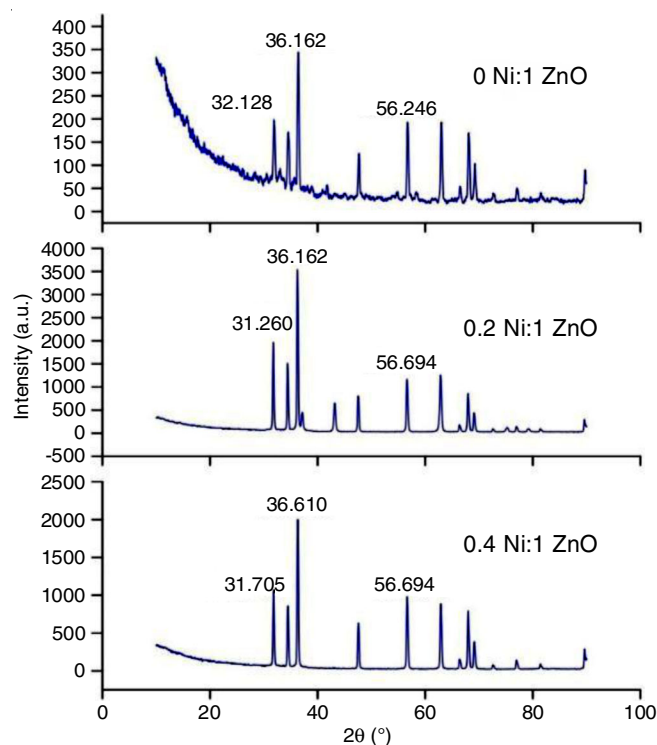


Fig. 1. XRD pattern of Ni-ZnO

to the (110) plane confirming the retention of the quartzite structure upon Ni doping. Peak broadening or in some cases splitting such as that between 31.260° and 31.705° could indicate doping-induced microstrain or variations in crystallite size. With the help of the Debye-Scherrer's formula, the average crystallite size can be calculated to ascertain the effects nanoparticle on the ZnO lattice. Also, there are no secondary phase peaks, which indicate the homogeneous incorporation of Ni ions without forming the segregated NiO phases, which further confirms the success of the doping process. The results indicate that Ni doping significantly alters the structural characteristics of ZnO, affecting both the capacity for Ni substitution to adjust lattice constants and the induction of strain, which in turn influences the crystallite size.

SEM analysis: The Ni doping may cause changes in the morphology; hence, depending on the method of synthesis and its doping level, various shapes and structures like spherical, rod or porous might be expected. The particle size distribution and grain boundaries generally govern the properties of $\text{Zn}_{1-x}\text{Ni}_x\text{O}$. In some cases, higher doping concentrations may yield finer grain sizes or aggregation, which would affect the electrical and optical characteristics. The SEM allows for detailed observation of surface roughness and texture. Variations in roughness can impact catalytical or sensor applications due to increased surface areas available for reactions. An EDS is often coupled to the SEM to trace the distribution of species, *e.g.*, Zn, Ni and O, in a material. This confirms homogeneous incorporation of Ni in the ZnO matrix and provides semi-quantitative data of elemental composition. Differences are observed between the undoped ZnO and $\text{Zn}_{1-x}\text{Ni}_x\text{O}$ bring forth understanding of the effects of Ni doping in microstructure, such as defect formation or phase separation that might influence it in turn with respect to optical, magnetic or electrical properties (Fig. 2).

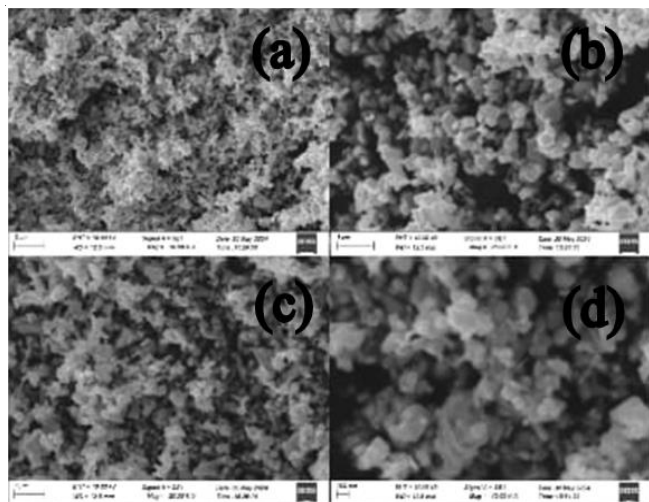


Fig. 2. SEM image of Ni-ZnO at different magnifications (a-d)

FTIR studies: FTIR spectroscopy is considered as a powerful tool for observing the chemical compositions and structural variations of nickel-doped zinc oxide ($\text{Zn}_{1-x}\text{Ni}_x\text{O}$) nanoparticles. The introduction of Ni^{2+} ions into the ZnO lattice occurs when zinc oxide doped with nickel nitrate. The mode of vibration

caused by stretching of the Zn-O bond appears at around $600\text{--}400\text{ cm}^{-1}$; doping with Ni^{2+} introduces a small shift in this area, attributed to changes in the lattice (Fig. 3). A separate peak possibly related to the Ni-O bond stretching vibration may arise at around $650\text{--}450\text{ cm}^{-1}$, supported by the addition of nickel. The FT-IR spectrum will then show a common feature of some shifts and new peaks related to the structural modification of the ZnO lattice incurred due to the substitution of Zn^{2+} with Ni^{2+} and the formation of new Ni-O bonds. These observed variations are some of the many changes to which insights into the bonding environment of the material and the electronic properties developed owing to nickel doping refined.

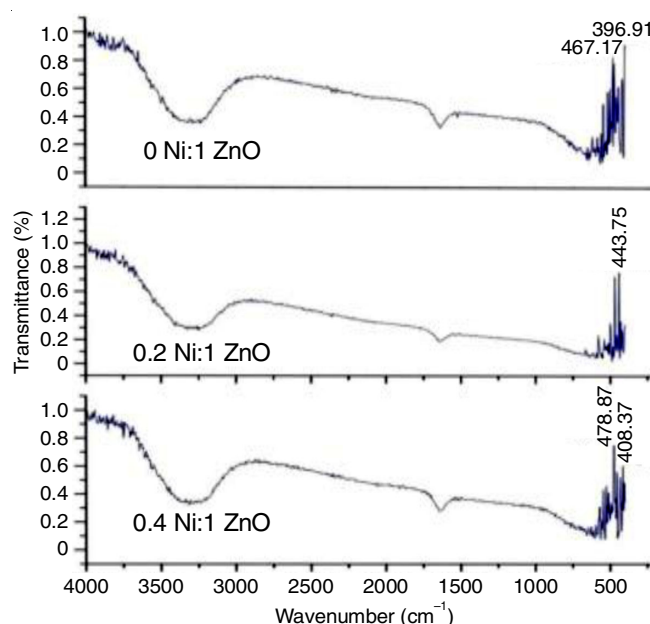


Fig. 3. FT-IR spectral studies of Ni-ZnO

Optical studies: Researchers often aim to explore the optical properties of $\text{Zn}_{1-x}\text{Ni}_x\text{O}$ by UV analysis in order to figure out the electrical structure of ZnO is affected by Ni doping, as well as its optical bandgap. The possible transitions connected with defects, impurities or changes in the band structure due to Ni doping usually reflect the colours of the peaks at 237.307 nm and 236.548 nm (Fig. 4). The slight differences in wavelengths may be attributed to alterations in optical characteristics resulting from varying Ni concentrations. The absorption spectrum could assist in finding the optical bandgap of $\text{Zn}_{1-x}\text{Ni}_x\text{O}$ based on the Tauc plot method. Typically, Ni doping leads to a decrease in the bandgap due to the introduction of Ni 3d states close to the conduction band. The influence of Ni concentration is attributed to the increasing Ni content in the material, suggesting that variations lead to alterations in absorption peaks, intensified the intensities or decreased bandgaps due to changes in band structure and an increase in defect states.

Photoluminescence: In photoluminescence (PL), the near-band-edge (NBE) emission, typically in the ultraviolet region, is associated with excitonic recombination at the conduction and valence bands. Doping with nickel often quenches or shifts this emission due to bandgap narrowing caused by the inter-

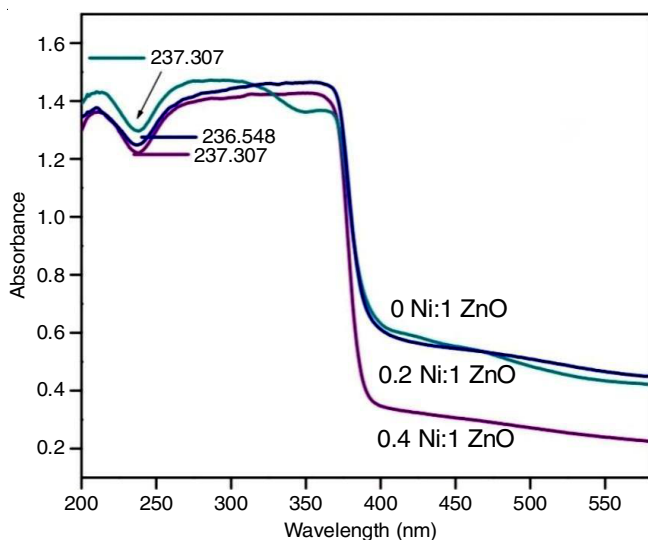


Fig. 4. UV-Vis spectrum of Ni-ZnO at different ratio

action of Ni ions with the host lattice. Additionally, the presence of defect-related emissions in the visible region, such as green, yellow or red light, can be attributed to intrinsic defects like oxygen vacancies or new dopant-induced states. The intensity and position of these emissions are highly sensitive to the doping concentration and synthesis conditions, such as calcination temperature and pH.

The presence of nickel can enhance or suppress certain defect emissions, offering control over the material's luminescent efficiency and functionality. The peak positions within 380 nm can provide insights into the defect density and the nature of the defect states introduced by nickel doping. Observing a redshift (movement of peak toward longer wavelengths) indicates a reduction in the bandgap (Fig. 5), which is consistent with in Ni-doped ZnO, the peak at 762 cm^{-1} in the PL spectrum is generally attributed to the effects of the dopants and crystal lattice defects. Ni doping introduces extra energy levels inside the bandgap of ZnO. These could be involved with intrinsic defect states such as oxygen vacancies or zinc interstitials. The interaction of Ni with other elements or states could either enhance or suppress luminescence in certain areas and the peak

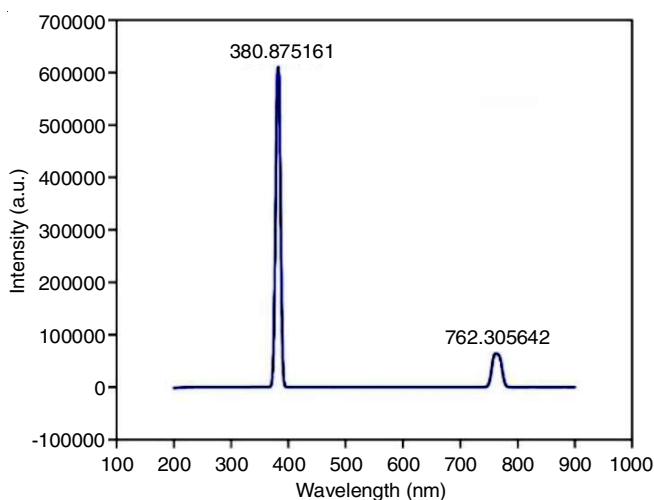


Fig. 5. Photoluminescence (PL) spectrum of Ni-ZnO

around 762 cm^{-1} possibly corresponds to transitions within defect states or acceptor pairs. Thus, it is verified through PL analysis of Ni-doped ZnO that nickel does indeed modify defect states in the material and the electronic properties.

Electrochemical studies: The redox activity of Ni-doped ZnO nanocomposite was observed. A sharp increase in current at approximately 1.5 V corresponds to oxidation, possibly due to Ni^{2+} going to Ni^{3+} , while the partial reduction of nickel ions back to Ni^{2+} shows a smaller plateau between 0 to -0.5 V (Fig. 6). The Faradaic process indicates that the electrochemical reaction arises from Faradaic charge storage linked to nickel ion redox transitions. Doping of nickel into zinc oxide increases the active sites, enhancing the charge-transfer kinetics. The quasi-rectangular shape of the capacitance nature in the low potential region -1 V to 0.5 V establishes that the capability is a double-layer capacitance (electrostatic charge adsorption) along with Faradaic pseudocapacitance (redox reactions from Ni centers). Increased current at the higher potential indicates an electrocatalytic effect, suggesting that nickel-doped ZnO has good electrocatalytic characteristics, especially in oxidation reactions. These materials thus have potential applications involving oxygen evolution reactions or energy storage. The incorporation of Ni within the ZnO lattice introduces localized electronic states which enhance conductivity and charge storage capacity. The high current response in the cyclic voltammetry (CV) study confirms the successful incorporation of nickel into zinc oxide. The CV results indicate that Ni-doped ZnO can be applied into energy storage devices: supercapacitors and batteries because of the redox activity and capacitive nature. Moreover, the high oxidative current responses can establish it as a potent electrocatalyst for the OER. Redox-sensitive properties indicate its also being effective for electrochemical sensors.

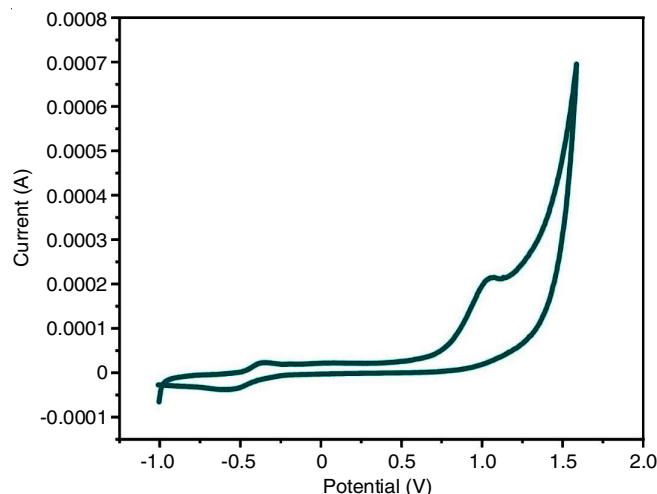


Fig. 6. Cyclic voltammogram of Ni-ZnO

Conclusion

Nickel nitrate-doped zinc oxide (Ni:ZnO) nanocomposites were synthesized and characterized successfully, revealing valuable insights into their structural, morphological, optical and electrochemical properties. Diffraction patterns showed

the traces of the hexagonal wurtzite structure of ZnO with minor shifts in peak positions, confirming successful incorporation of the Ni ions into the ZnO lattice. The crystallite size decreased slightly due to the incorporation of Ni, which can be ascribed to some extent of lattice distortion owing to Ni substitution. Morphological studies revealed that the synthesized nanocomposites had quite uniform morphology with well-defined nanoparticles. The influence of the Ni substitution in the agglomeration behaviour and surface texture of the ZnO particles seemed to further enable better dispersion in the composite matrix. The FTIR confirmed the presence of characteristic Zn–O stretching vibrations in the wavelength range along with few extra peaks attributed to Ni–O and nitrate groups. The Zn–O peaks after doping were also found to disappear somewhat and broaden, indicating successful incorporation of Ni. Optical spectroscopy demonstrated the Ni-doped ZnO nanocomposite shifting of the band gap energy. The red shift suggests the localization of energy states within the ZnO band structure, providing the enhancement in its optical properties. Photoluminescence studies showed an overall decreased emission intensity, which means the competition for recombination between electrons and holes occurring in that support is much less, thus favouring their photocatalytic and optoelectronic applications. Electrochemical analysis (cyclic voltammetry) exhibited the electrochemical activity of the Ni:ZnO nanocomposites. Enhanced redox peak currents and better transport properties for charge were observed, assigned to the synergistic effect of Ni doping. These results substantiate these nanocomposites for energy storage devices and sensing. Overall performance and potential applications the introduction of nickel nitrate to ZnO nanoparticles further leads to their improved stability, optical tunability and electrochemical performance.

CONFLICT OF INTEREST

The authors declare that there is no conflict of interests regarding the publication of this article.

REFERENCES

1. Y. Zhang and X. Xu, *ACS Omega*, **5**, 15344 (2020); <https://doi.org/10.1021/acsomega.0c01438>
2. R. Kant, V. Ahuja, K. Joshi, H. Gupta and S. Bhardwaj, *Vacuum*, **204**, 111375 (2022); <https://doi.org/10.1016/j.vacuum.2022.111375>
3. A. Rajeh, H.A. Althobaiti, S.J. Almeahmadi, H.A. Alsalmah, N.A. Masmali, A.I. Al-Sulami and M. Al-Ejji, *J. Inorg. Organomet. Polym. Mater.*, **34**, 1221 (2024); <https://doi.org/10.1007/s10904-023-02880-w>
4. S.P. Vattikuti, J. Shim, N. Nguyen Dang, P. Rosaiah, M.R. Karim, I.A. Alnaser and B. Khan, *Int. J. Energy Res.*, **2024**, 4589047 (2024); <https://doi.org/10.1155/2024/4589047>
5. S.G. Danjumma, Y. Abubakar and S. Suleiman, *J. Eng. Res. Technol.*, **8**, 12 (2019).
6. S.D. Dhas, P.S. Maldar, M.D. Patil, A.B. Nagare, M.R. Waikar, R.G. Sonkawade and A.V. Moholkar, *Vacuum*, **181**, 109646 (2020); <https://doi.org/10.1016/j.vacuum.2020.109646>
7. K.O. Ukoba, A.C. Eloka-Eboka and F.L. Inambao, *Renew. Sustain. Energy Rev.*, **82**, 2900 (2018); <https://doi.org/10.1016/j.rser.2017.10.041>
8. K. Davis, R. Yarbrough, M. Froeschle, J. White and H. Rathnayake, *RSC Adv.*, **9**, 14638 (2019); <https://doi.org/10.1039/C9RA02091H>
9. A.B. Djurišić and Y.H. Leung, *Small*, **2**, 944 (2006); <https://doi.org/10.1002/sml.200600134>
10. D.K. Sharma, S. Shukla, K.K. Sharma and V. Kumar, *Mater. Today Proc.*, **49**, 3028 (2022); <https://doi.org/10.1016/j.matpr.2020.10.238>
11. K. Jayaraman, M. Kotaki, Y. Zhang, X. Mo and S. Ramakrishna, *J. Nanosci. Nanotechnol.*, **4**, 52 (2004).
12. I. Stolyarchuk, O. Kuzyk, O. Dan'kiv, A. Dziedzic, G. Kleto, A. Stolyarchuk, A. Popovych and I. Hadzaman, *Coatings*, **13**, 601 (2023); <https://doi.org/10.3390/coatings13030601>
13. A. Janotti and C.G. Van de Walle, *Rep. Prog. Phys.*, **72**, 126501 (2009); <https://doi.org/10.1088/0034-4885/72/12/126501>
14. S. Minisha, J. Johnson, S. Mohammad, J.K. Gupta, S. Aftab, A.A. Alothman and W.C. Lai, *Water*, **16**, 340 (2024); <https://doi.org/10.3390/w16020340>
15. F. Ahmed, N. Arshi, M.S. Anwar, S.H. Lee, E.S. Byon, N.J. Lyu and B.H. Koo, *Curr. Appl. Phys.*, **12**, S174 (2012); <https://doi.org/10.1016/j.cap.2012.02.054>
16. A.K. Azfar, M.F. Kasim, I.M. Lokman, H.A. Rafaie and M.S. Mastuli, *R. Soc. Open Sci.*, **7**, 191590 (2020); <https://doi.org/10.1098/rsos.191590>
17. I.B. Elkamel, N. Hamdaoui, A. Mezni, R. Ajjel and L. Beji, *RSC Adv.*, **8**, 32333 (2018); <https://doi.org/10.1039/C8RA05567J>
18. S.H. Zyoud, V. Ganesh, C.A. Che Abdullah, I.S. Yahia, A.H. Zyoud, A.F. Abdelkader, M.G. Daher, M. Nasor, M. Shahwan, H.Y. Zahran, M.S. Abd El-Sadek, E.A. Kamoun, S.M. Altarifi and M.S. Abdel-Wahab, *Crystals*, **13**, 1087 (2023); <https://doi.org/10.3390/cryst13071087>
19. S. Ahmad, M. Usman, M. Hashim, A. Ali, R. Shah and N.U. Rahman, *Nanomater. Nanotechnol.*, **2024**, 8330886 (2024); <https://doi.org/10.1155/2024/8330886>
20. R.N. Ali, H. Naz, J. Li, X. Zhu, P. Liu and B. Xiang, *J. Alloys Compd.*, **744**, 90 (2018); <https://doi.org/10.1016/j.jallcom.2018.02.072>
21. N. Guermat, W. Daranfed, I. Bouchama and N. Bouarissa, *J. Mol. Struct.*, **1225**, 129134 (2021); <https://doi.org/10.1016/j.molstruc.2020.129134>
22. R. Elilarassi and G. Chandrasekaran, *Optoelectron. Lett.*, **6**, 6 (2010); <https://doi.org/10.1007/s11801-010-9236-y>
23. R. Elilarassi and G. Chandrasekaran, *J. Mater. Sci. Mater. Electron.*, **22**, 751 (2011); <https://doi.org/10.1007/s10854-010-0206-8>
24. V. Vijayaprasath, R. Murugan, S. Palanisamy, N.M. Prabhu, T. Mahalingam, Y. Hayakawa and G. Ravi, *Mater. Res. Bull.*, **76**, 48 (2016); <https://doi.org/10.1016/j.materresbull.2015.11.053>